BBA - Reviews on Cancer 1871 (2019) 367–378

Contents lists available at ScienceDirect

BBA - Reviews on Cancer

journal homepage: www.elsevier.com/locate/bbacan

Review

Atomic force microscopy-based cancer diagnosis by detecting cancer-specific biomolecules and cells

Taeyun Kwon[a,*], Sundaram Gunasekaran[b], Kilho Eom[c,*]

[a] SKKU Advanced Institute of Nano Technology (SAINT), Sungkyunkwan University (SKKU), Suwon 16419, Republic of Korea
[b] Department of Biological Systems Engineering, and Department of Materials Science & Engineering, University of Wisconsin-Madison, 460 Henry Hall, Madison, WI 53706, USA
[c] Biomechanics Laboratory, College of Sport Science, Sungkyunkwan University (SKKU), Suwon, 16419, Republic of Korea

ARTICLE INFO

Keywords:
Atomic force microscopy (AFM)
Cancer
Biomolecule/cell detection
Imaging
Cantilever
Biomolecular interactions
Cancer progression

ABSTRACT

Atomic force microscopy (AFM) has recently attracted much attention due to its ability to analyze biomolecular interactions and to detect certain biomolecules, which play a crucial role in disease expression. Despite recent studies reporting AFM imaging for the analyses of biomolecules, the application of AFM-based cancer-specific biomolecule/cell detection has remained largely underexplored, especially for the early diagnosis of cancer. In this paper, we review the recent attempts, including our efforts, to analyze and detect cancer-specific biomolecules and cancer cells. We particularly focus on two AFM-based cancer diagnosis techniques: (i) AFM imaging-based biomolecular and cellular detection, (ii) AFM cantilever-based biomolecular sensing and cell analysis. It is shown that AFM-based biomolecular detection has been applied for not only early diagnosing cancer, by measuring the minute amount of cancer-specific proteins, but also monitoring of cancer progression, by correlating the amount of cancer-specific proteins with the progression of cancer. In addition, AFM-based cell imaging and detection have been employed for diagnosing cancer, by detecting cancerous cells in tissue, as well as understanding cancer progression, by characterizing the dynamics of cancer cells. This review, therefore, highlights AFM-based biomolecule/cell detection, which will pave the way for developing a fast and point-of-care diagnostic system for biomedical applications.

1. Introduction

Cancer is one of fatal diseases that critically reduce the life expectancy of people in the world. According to the report, in 2015, there were 90.5 million people who had suffered from cancer [1], and about 14.1 million new cases occurred a year (with excluding skin cancer other than melanoma) [2]. In addition, cancer is a disease of long history even dated back to 1500 BCE, in which written was a papyrus that described eight cases of tumors occurring in the breast. Cancer originates from the abnormal growth of cells that acquired the cancer-promoting gene mutations [3]. These cells undergoing abnormal growth due to cancer-promoting gene mutation are referred to as cancer cells. For cancer diagnosis, therefore, it is of high significance to characterize the properties of cancer cells and/or biomolecules specifically expressed on cancer cells. For example, specific proteinase (e.g. matrix metalloproteinase) are expressed on cancer cells in order to foster the abnormal growth of cancer cells [4], which indicates the possibility of cancer diagnosis by detecting and characterizing such proteinases and their activity.

For recent decade, nanotechnology has played a vital role in establishing a de novo cancer diagnostics [5] by detecting cancer cells and/or cancer-specific biomolecules. Specifically, the advancement of nanotechnology has led to the emergence of small-scale devices such as micro-electro-mechanical systems (MEMS) and nano-electro-mechanical systems (NEMS), which have enabled the understanding and analysis of biomolecular interactions [6–9]. For instance, researchers in Switzerland [10] reported the nanomechanical cantilever-based sensitive detection of disease-specific DNA molecules based on the hybridization of disease-specific DNA molecules and probe molecules functionalized on a cantilever's surface. This small-scale nanomechanical device, which is able to sense and detect disease-specific biomolecules, has played a role in not only diagnosis of diseases such as cancers but also evaluation of the efficacy of newly designed drug molecules.

Atomic force microscopy (AFM) is now a commercially available toolkit for studying biological [11] and nanoscale entities [12], and

* Corresponding authors.
E-mail addresses: taeyunkwon@skku.edu (T. Kwon), kilhoeom@skku.edu (K. Eom).

https://doi.org/10.1016/j.bbcan.2019.03.002
Received 30 January 2019; Received in revised form 21 March 2019; Accepted 26 March 2019
Available online 02 April 2019
0304-419X/

allows for imaging specific surfaces at atomic scale [13] and measuring physical quantities such as surface charges [14,15] and mechanical properties [16–18]. While the ability of scanning electron microscopy (SEM) and tunneling electron microscopy (TEM) is limited to imaging only conductive objects, AFM has the ability to visualize non-conductive objects such as polymers and soft matters (e.g. biomolecules and cells). The basic principle of AFM imaging is to measure the change in bending deflection or resonant frequency of an AFM cantilever (i.e. force probe) due to the interaction between the cantilever tip and the surface being measured.

AFM imaging techniques have recently been widely utilized for studying the interactions and detection of biomolecules. For instance, AFM imaging has allowed for understanding the interaction between lac repressor and λ-DNA molecule and the conformations of lac repressor-bound λ DNA molecule [19]. Recently, Kelvin probe force microscopy (KPFM) imaging has been employed for quantitative analysis of biomolecular interactions based on the measurement of change in surface charge due to biomolecular interactions [20]. We reported KPFM imaging-based analysis of the efficacy of drug molecules that inhibit ATP-binding onto protein kinase [21]. The resolution of AFM imaging has been improved by using a specialized AFM cantilever tip such as T-shaped torsional cantilever [22]. Here, we note that AFM imaging is useful in detecting cancer-specific biomolecules when compared with other conventional approaches as follows: (i) While other imaging-based detection method (e.g. fluorescence imaging) usually requires the labeling process that is cumbersome, AFM allows for imaging specific biomolecules (with high resolution even up to single-molecule resolution) without any labeling or chemical modification. (ii) AFM enables the highly sensitive detection of cancer-specific biomolecules. For example, the detection limit of AFM-based diagnosis is as low as 1 pM, which is much lower than the detection limit of conventional approaches. (iii) KPFM imaging coupled with AFM imaging allows for imaging the electrostatic properties of biomolecules, which are useful in recognition of interaction between small molecule (e.g. ATP, drug, etc.) and cancer-specific protein. Conventional approaches are unable to characterize the interaction between small molecule and cancer-specific protein, while KPFM is able to do. Thus, we expect that AFM/KPFM will serve as a diagnostic toolkit that enables the analysis and detection of single biomolecules.

Cantilevers that serve as a probe for AFM imaging have been also employed for highly sensitive detection of disease-specific biomolecules [23–29]. As mentioned earlier, the AFM cantilever has been successful in detecting disease-specific DNA molecules based on the bending deflection change or frequency shift of the cantilever [10,30–32]. In addition, the vibrating AFM cantilever is used to measure the mass of disease-specific biomolecules that bind to the cantilever [28,33], since the resonant frequency of a cantilever is inversely proportional to the square root of the overall mass of the cantilever. Based on this, researchers have reported the highly sensitive label-free detection of biomolecules such as proteins [33–35], RNA [36], and enzymes [37–39].

Herein, we review the recent efforts to analyze and detect cancer-specific biomolecular interactions and cancer cells using AFM-based biomolecule/cell imaging as well as resonant AFM cantilever sensor (Fig. 1).

2. Principles

2.1. Atomic force microscopy-based imaging

The basic principle of AFM imaging is to visualize the surface of a sample by measuring the force between the AFM probe (i.e. cantilever tip) and the sample based on the bending deflection of the cantilever tip due to such a force. As shown in Fig. 2, AFM is composed of a probe, laser, scanner, photodetector and data collector. The AFM cantilever tip allows for acquiring the images and chemical, physical, and biological information of the sample when the cantilever tip transverses the sample surface (Fig. 2). According to Hooke's law, for small deflection, the extent of cantilever deflection (x) is proportional to the bending force (F):

$$F = kx \tag{1}$$

where k is the stiffness of cantilever.

AFM imaging is commonly performed in two modes: (i) contact mode and (ii) tapping mode (Fig. 2). In contact mode, imaging is based on the contact between AFM cantilever tip and the surface that is being imaged. When AFM cantilever tip moves in a contact with the surface, the tip motion modulated by the surface morphology is optically measured in such a way that the motion of cantilever tip changes the reflection of laser focused on the surface of a cantilever. In tapping mode, imaging is based on measuring the resonant frequency of AFM cantilever tip, which is affected by tip-surface interaction. Typically, the tapping mode is appropriate for imaging soft matter, such as biomolecules and cells, which can be easily torn or fractured by the tip [40,41].

2.2. Kelvin probe force microscopy-based imaging

The basic principle of KPFM imaging is to measure the force acting on a vibrant AFM cantilever tip due to electrical charges on the surface of a nanoscale object (e.g. biomolecule). Since some amino acids of biomolecule possess surface electrical charges, the KPFM imaging is useful in visualizing and measuring the surface charges of such nanoscale objects [14,20]. Surface charge is an important parameter that determines the structure and function of a biomolecule. For instance, electrostatic interaction plays a key role in protein folding [42] and protein aggregation [43–45], which is responsible for pathogenesis of neurodegenerative diseases [46–48]. Thus KPFM imaging technique may lead the way to study the charge characteristics of a disease-specific biomolecule.

Since the sample surface and the cantilever tip constitutes a capacitive system, the energy stored in a capacitor (U_{cap}) is given by

$$U_{cap} = \frac{1}{2}C(\Delta V)^2 \tag{2}$$

where C is the capacitance of a system composed of the sample and the AFM cantilever tip, and ΔV is the difference in electrical potentials between the sample surface and the AFM cantilever tip. The force (F) acting on a cantilever can be obtained by differentiation of U_{cap} with respect to the distance (Z) between the sample surface and the AFM cantilever tip. That is,

$$F = -\frac{dU_{cap}}{dZ} = -\frac{1}{2}\frac{dC}{dZ}(\Delta V)^2 \tag{3}$$

Here, ΔV can be separated into DC and AC term as follows.

$$\Delta V = \Delta V_{DC} + \Delta V_{AC}\sin(\omega_{KP}t) \tag{4}$$

where ω_{KP} is the frequency applied to the probe tip. When $(\Delta V)^2$ is expanded, we have following three terms.

$$(\Delta V)^2 = \left[(\Delta V_{DC})^2 + \frac{(\Delta V_{AC})^2}{2}\right] - \frac{1}{2}(\Delta V_{AC})^2\cos(2\omega_{KP}t) + 2(\Delta V_{DC})(\Delta V_{AC})\sin(\omega_{KP}t) \tag{5}$$

When the frequency (ω_{KP}) is chosen to be the resonant frequency of the cantilever tip, the last term (i.e. ω_{KP} term) in Eq. (5) will dominate the force response of capacitor. This leads to the force acting on the cantilever tip as follows.

$$F = -\frac{dC}{dZ}\Delta V_{DC}\Delta V_{AC}\sin(\omega_{KP}t) \tag{6}$$

Here, it should be noted that ΔV_{DC} is given in the following form: $\Delta V_{DC} = \Delta V_{DC,app} - \Delta\phi$, where $\Delta\phi$ is the difference in surface potential

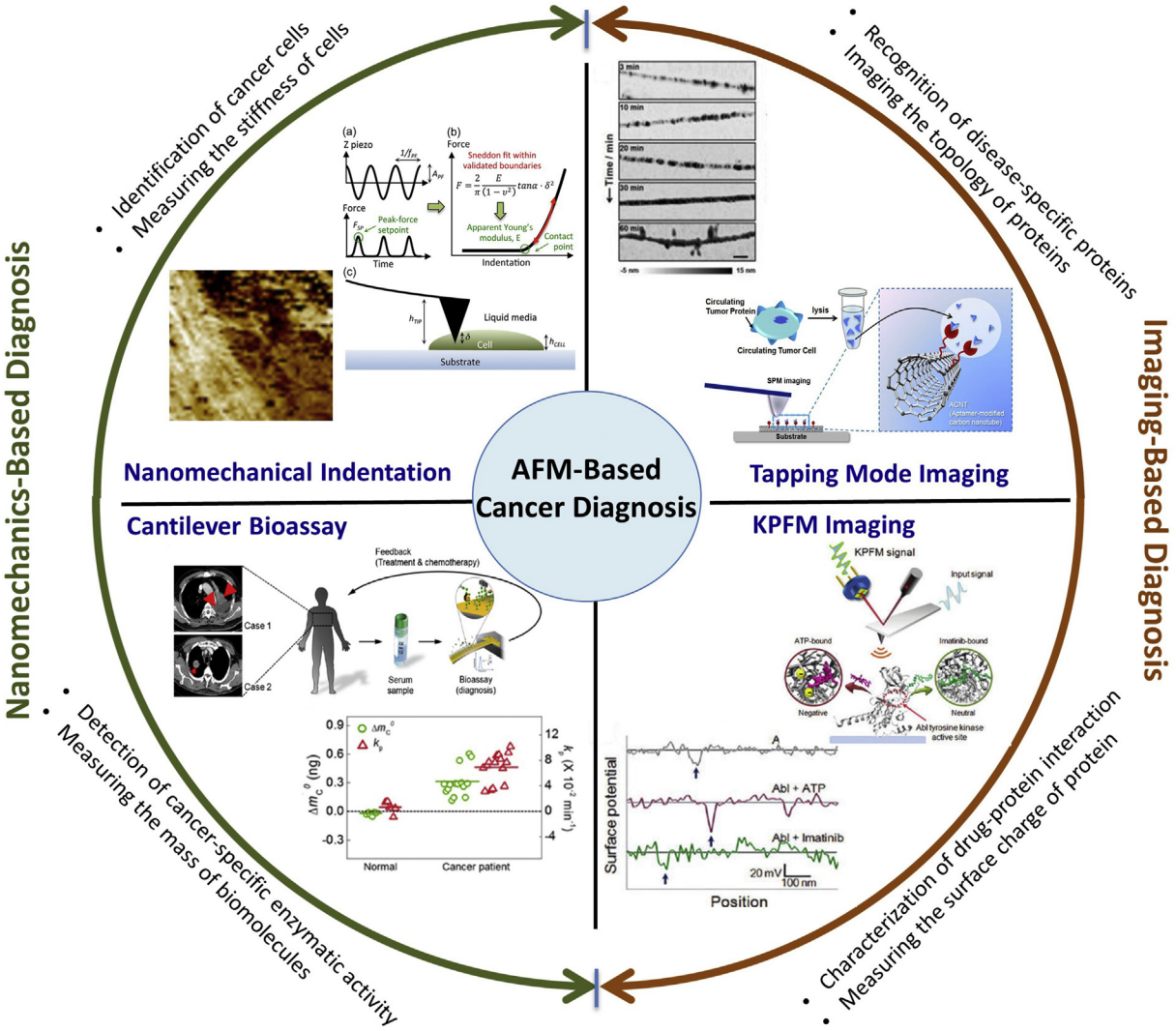

Fig. 1. Schematic illustration of AFM-based cancer diagnosis, which can be categorized into AFM imaging-based diagnosis and AFM nanomechanics-based diagnosis. For AFM imaging-based diagnosis, cancer-specific biomolecules (via AFM imaging) and their surface charge (via KPFM imaging) can be imaged and detected. For AFM nanomechanics-based diagnosis, the physical (i.e. mechanical) properties of cancer cells can be measured and imaged (i.e. via AFM nanomechanical mapping) or the mass of molecules (e.g. peptides cleaved by matrix metalloproteinase) and cancer cells can be estimated (via vibrant cantilever sensor). Figures are adopted with permission from Ref. [21, 66, 80] and adopted from Ref. [91] under Creative Commons Attribution License.

charges between the cantilever tip and sample surface. From Eq. (6), it is straightforward to compute $\Delta\phi$ if F is measured.

2.3. Nanomechanical mapping

Nanomechanical mapping (NMM) allows for measuring the mechanical properties of a sample by mechanically indenting it. The contact mechanics theory provides a relationship between the indentation force (F) and indentation depth (d) of the sample. For an elastic contact between AFM tip and sample (i.e. for small d without any adhesion), Hertz theory [49] suggests

$$d = \left(\frac{9F^2}{16E_{eff}^2 R_{eff}}\right)^{\frac{1}{3}} \tag{7}$$

where

$$\frac{1}{E_{eff}} = \frac{1-\nu_T^2}{E_T} + \frac{1-\nu_S^2}{E_S} \text{ and } \frac{1}{R_{eff}} = \frac{1}{R_T} + \frac{1}{R_S}$$

Here, E_{eff} is effective elastic modulus, R_{eff} is effective radius of curvature, E is elastic modulus, ν is Poisson's ratio, R is radius of curvature, and subscripts T and S represent the AFM tip and sample, respectively.

For an elastic, adhesive contact between AFM tip and sample, Johnson-Kendall-Roberts (JKR) theory provides the relationship between d and F such as [49]

$$d = \left[\frac{3F + 18\pi\gamma + 3\sqrt{12\pi\gamma R_{eff} + (6\pi\gamma R_{eff})^2}}{4E_{eff}\sqrt{R_{eff}}}\right]^{\frac{2}{3}}$$

Here, γ is a surface energy associated with adhesive contact, which is given as $\gamma = P/3\pi R_{eff}$ with P being a pull-off force. NMM based on Hertz theory or JKR theory enables one to measure the elastic modulus (and/or adhesive force) of a sample.

AFM-based NMM provides the high-resolution maps of modulus and adhesion force for biological samples such as cells simultaneously by scanning their surface [50,51]. NMM has been extensively employed for evaluating the mechanical properties of cells including cancer cells [52–54]. When cancer cells progress from a static phenotype to a metastatic phenotype, the physical properties of cells change due to the rearrangement of cytoskeleton network [55]. This change of physical properties caused by biological changes can be measured by NMM for cancer diagnosis.

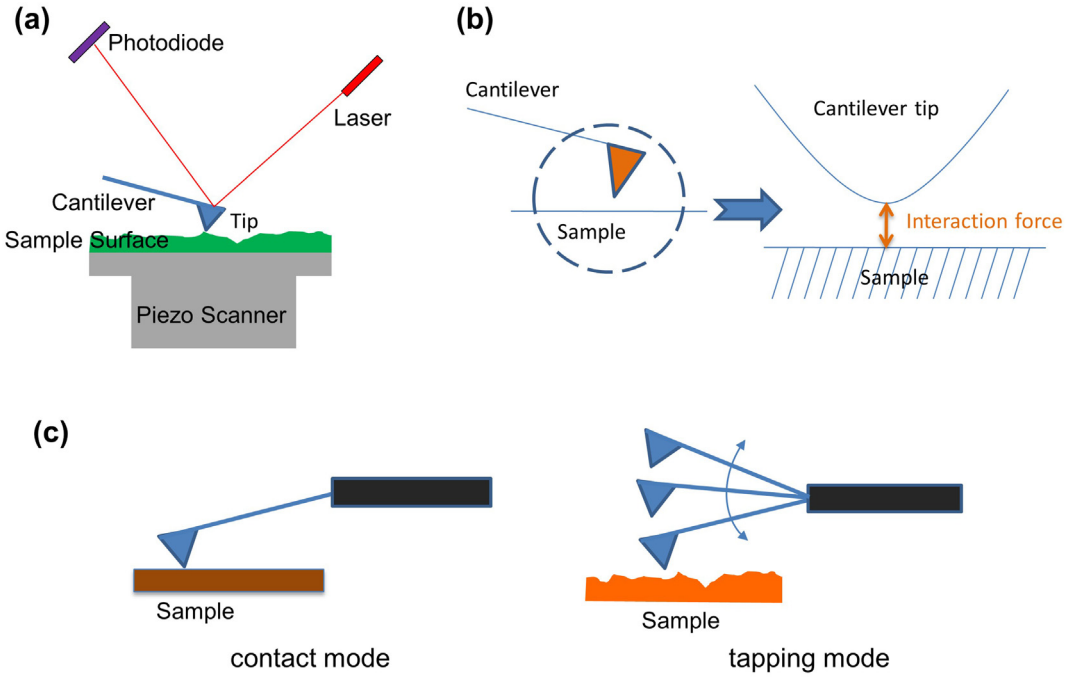

Fig. 2. Schematic illustration of AFM imaging. (a) Main components of AFM instrument. (b) Principles of AFM imaging based on the interaction between AFM tip and sample surface. (c) Two types of AFM imaging techniques, one of which is contact mode imaging (left), while the other is tapping mode imaging (right).

2.4. Vibrant cantilever-based detection

The equation of motion for a vibrating cantilever is given by [28]

$$\mu\partial_t^2 w(x,t) + D\partial_x^4 w(x,t) = 0 \tag{8}$$

where $w(x, t)$ is the bending deflection of a cantilever as function of its longitudinal coordinate x and time t, and μ and D are mass per length and bending rigidity of the cantilever, respectively. For a vibrant cantilever, $w(x, t) = u(x)\cdot\exp[j\omega t]$, where ω and $u(x)$ represent the resonant frequency of a cantilever and its related bending deflection mode, respectively, and $j = \sqrt{-1}$. Then, based on Eq. (8), the resonant frequency (ω) of a cantilever is given by

$$\omega = \left(\frac{\lambda}{L}\right)^2\sqrt{\frac{D}{\mu}} \tag{9}$$

where L is the length of a cantilever, and λ is a constant that satisfies a transcendental equation such as $\cos\lambda\cdot\cosh\lambda + 1 = 0$. When biomolecules are adsorbed onto a cantilever, its resonant frequency decreases, while the bending rigidity remains unaffected, since the elastic modulus of a cantilever is about four orders of magnitude larger than that of a biomolecule. The resonant frequency of a cantilever with biomolecular adsorption is

$$\omega' = \left(\frac{\lambda}{L}\right)^2\sqrt{\frac{D}{\mu + \Delta\mu}} \tag{10}$$

where $\Delta\mu$ is the change in mass per length due to adsorbed biomolecules such as $\Delta\mu = \Delta m/L$ with Δm being the total mass of adsorbed biomolecules. From Eqs. (9) and (10), the total mass of biomolecules that attach to a cantilever is calculated as

$$\Delta m = \lambda^4\frac{D}{L^3}\left(\frac{1}{\omega'^2} - \frac{1}{\omega^2}\right) \tag{11}$$

3. Atomic force microscopy imaging-based cancer diagnosis

AFM-based imaging and detection of biomolecules have been receiving attention, as AFM enables the recognition of disease-specific biomolecules at molecular level. Conventional imaging methods, such as fluorescence imaging, must involve chemical modification such as labeling that affects the chemical environment of the molecule, which interferes with precisely observing actual interactions between molecules [56]. However, non-contact (i.e. tapping) mode AFM imaging allows direct mapping without altering the structure of biomolecules [57]. Mazzola et al. [56] used a photolithography technique to create a biotin-streptavidin array on a substrate, and then succeeded in AFM-based label-free imaging of biomolecules. Henderson et al. [58] detected a virus particle by using a protein array-coated surface coupled with tapping mode AFM imaging.

The sensitivity of AFM-based biomolecular detection can be improved by surface patterning that allows for capturing the target biomolecule in a minimal sensing area, which has been accomplished via dip pen nanolithography (DPN) [59] or aligned carbon nanotubes (CNTs) [60], which has been shown to improve the detection limit of AFM imaging-based biomolecular detection. For instance, aligned CNTs-patterned surface has enabled the sensitive detection of marker proteins at concentrations of < 1 pM. Cancer-specific marker proteins expressed in cancer cells have been sensitively detected for effective early diagnosis of cancer. For early diagnosis of cancer, it is essential to detect and trace a small amount of carcinoembryonic antigens (CEAs) expressed in few circulating tumor cells (CTCs) [61–63], specifically, CEAs (or CTCs) at concentration of ~2.5 ng/mL (or 1–10 CTCs per mL) [64,65]. For highly sensitive detection of protein molecules, Kwon et al. [60] considered a surface where individual CNTs are horizontally aligned over the sensing area. When target biomolecules attach to the CNTs, the height and surface roughness of the CNTs increase. Accordingly, the CNTs-patterned surface coupled with AFM imaging has been used for highly sensitive detection of CEAs expressed on few CTCs [66]. Here, to specifically capture CEAs, the surface of CNTs was chemically modified using aptamers as receptor molecules. It is shown that CNTs-patterned surface coupled with AFM imaging enables the sensitive, label-free detection of CEA-related cell-adhesion molecule 5 (CEACAM5) expressed on CTC cells with the detection sensitivity of 0.001 cells/mL, or equivalently 20 CEACAM5 molecules per micrometer in CNT (Fig. 3). In addition, AFM imaging provides the time-dependent number of CEACAM5 molecules bound to CNTs-patterned

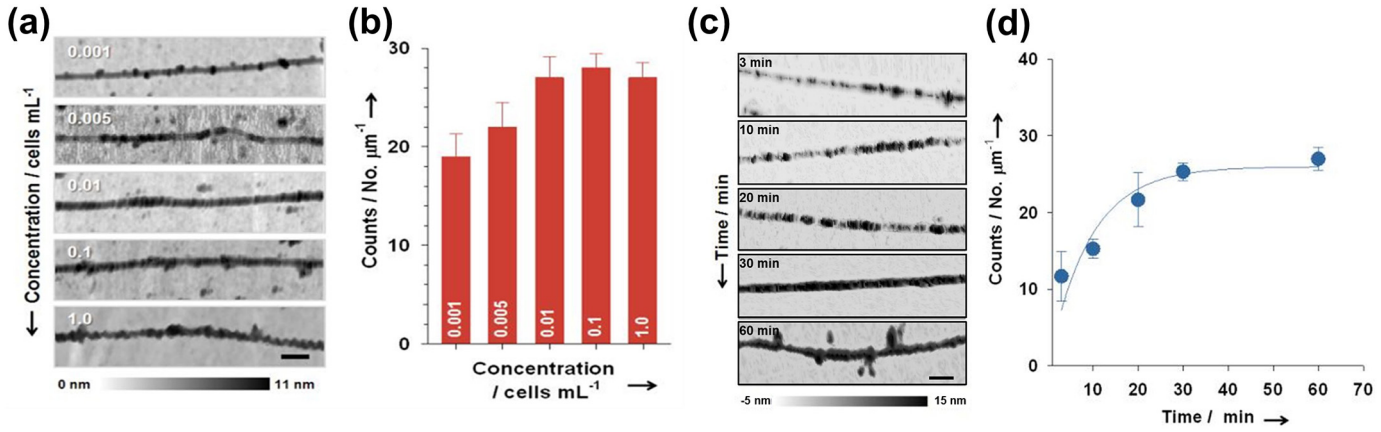

Fig. 3. AFM imaging-based sensitive detection of cancer-specific proteins, i.e. CEACAM5 proteins expressed on circulating tumor cell (CTC). (a) AFM topographic images of CEACAM5 proteins (black dots) bound to carbon nanotube (CNT) patterned on a surface. (b) Number of CEACAM5 proteins bound to CNT as a function of CTC concentration. (c) AFM topology images of CEACAM5 proteins bound to CNT with respect to time. (d) Number of CEACMA5 proteins captured by CNT as a function of time. The scale bar is 100 nm. Figure is adopted with permission from Ref. [66].

surface, which can be depicted by Langmuir kinetics.

$$N(t) = N_0[1 - \exp(-k_b t)] \quad (12)$$

where $N(t)$ is the time-dependent number of CEACAM5 molecules bound to CNTs, N_0 is the equilibrium value of the number of CEACAM5 molecules captured by CNTs, and k_b is a rate constant for binding between CEACAM5 and CNT surface. Here, it should be noted that the time constant for binding (τ) is given by $\tau = 1/k_b$. The kinetic rate for binding between CEACAM5 and aptamer-modified CNT surface was found to be 0.06 min^{-1}, which is equivalent to the time constant for binding being 16.67 min. This implies that CNTs-patterned surface coupled with AFM imaging allows fast and acute cancer diagnosis.

4. Kelvin probe force microscopy imaging-based cancer diagnosis

For sensitive, label-free imaging and detection of biomolecules, a surface patterning based on DPN [67] or nanomaterial (e.g. CNT) is useful. One of examples for KPFM imaging coupled surface patterning is the visualization of DNA molecules that are bound to probe DNA molecules patterned by DPN [68]. This is attributed to the fact that the backbone of DNA molecule bears negative charges that can be imaged by KPFM. The surface charge of hybridized DNA molecule (i.e. double-stranded DNA molecule) is twice as large as that of a probe DNA (i.e. single-stranded DNA). Here, we note that though the surface patterning is useful for KPFM imaging-based sensitive biomolecular detection, the surface patterning is not always required at all.

KPFM has been highlighted due to its capability of not only detecting specific biomolecules but also characterizing the interaction between specific protein and small ligand (such as ATP or drug molecule). In our previous study [21], it is shown that KPFM imaging allows for quantitatively characterizing the interaction between protein kinase (e.g. Abl tyrosine kinase) and small ligand. In particular, we showed that AFM imaging is unable to distinguish unbound wild type protein kinase from ATP-bound protein kinase (or drug-bound protein kinase), because the ligand (e.g. ATP or drug molecule) is much smaller than the spatial resolution of AFM imaging. On the other hand, KPFM imaging is capable of label-free recognition of protein kinase in different states such as unbound state, ATP-bound state, and drug-bound state, since protein kinase is each state exhibits the different charge state due to the fact that ATP exhibits the negative charge, while drug molecule (e.g. imatinib) is electrostatically neutral. It is remarkably shown that KPFM imaging enables the precise recognition of protein kinase in unbound, ATP-bound, or drug-bound state with single-molecule resolution (Fig. 4). Our previous work [21] highlights the use of KPFM imaging to quantify the efficacy of a drug molecule, suggesting the application of KPFM imaging for drug-screening at single-molecule level.

Lee et al. [69] reported the ability of KPFM imaging coupled with DNA-capped nanoparticle (DCNP) to sensitively detect the genetic mutation of cancer-specific DNA sequence. The nanoparticles functionalized with probe DNA, which are able to capture the specific target DNA (e.g. cancer-specific DNA), were used as surface charge amplifier for KPFM imaging. Lee et al. considered the wild type (WT) and mutant BRCA1 gene (responsible for breast and/or ovarian cancer) as a target DNA. When the target BRCA1 gene was bound to DCNP, the surface charge of DCNP changed due to the negative charge of the target DNA. The ability of KPFM imaging to discriminate WT BRCA1 gene from its mutant was shown to be due to the negative charge of WT BRCA1 DNA being different from that of BRCA1-mutant DNA. They showed that DCNP capturing WT BRCA1 DNA exhibits higher surface charge state than DCNP interacting with BRCA1-mutant DNA. This work suggests the possibility of KPFM imaging to detect genetic information of cancer-specific DNA such as single-nucleotide polymorphism (SNP). Similarly, Jang et al. [70] reported the ability of KPFM coupled with DCNP to detect cancer-specific DNA sequence, i.e. DNA sequence for Kirsten rat sarcoma viral oncogene homolog (KRAS) and epidermal growth factor receptor (EGFR). They showed that DCNP interacting with KRAS-mutant DNA exhibits higher surface potential than DCNP bound with WT KRAS DNA. They have also shown that KPFM imaging coupled with DCNP allows for detecting EGFR-specific DNA molecules even at a concentration ~3 pM.

5. Nanomechanical mapping-based cancer diagnosis

As the shape of early cancer cells is very similar to that of normal cells, it is very difficult to distinguish them morphologically; however, their mechanical properties have subtle differences [71,72], which AFM can help distinguish. AFM-based mechanical indentation (i.e. NMM) has been used to recognize the metastatic cancer cells obtained from the body fluids of patients suffering from various cancers such as lung cancer, breast cancer, and pancreas cancer. For example, Gimzewski et al. [73] reported that the stiffness (Young's modulus, E) of cancer cells, measured from the force-displacement curves acquired from AFM-based indentation experiment, is > 70% less than that of benign cells that line the body cavity.

NMM measurements of elastic properties of biological samples has been used for cancer diagnosis [74,75]. Geahlen et al. [76] mapped the nanomechanical properties of live MDA-MB-231 breast cancer cells either lacking or expressing Syk (spleen kinase) proteins by using multi-harmonic AFM. Here, Syk, a modulator of immune recognition receptor signaling, plays important roles in tumor progression and inhibits

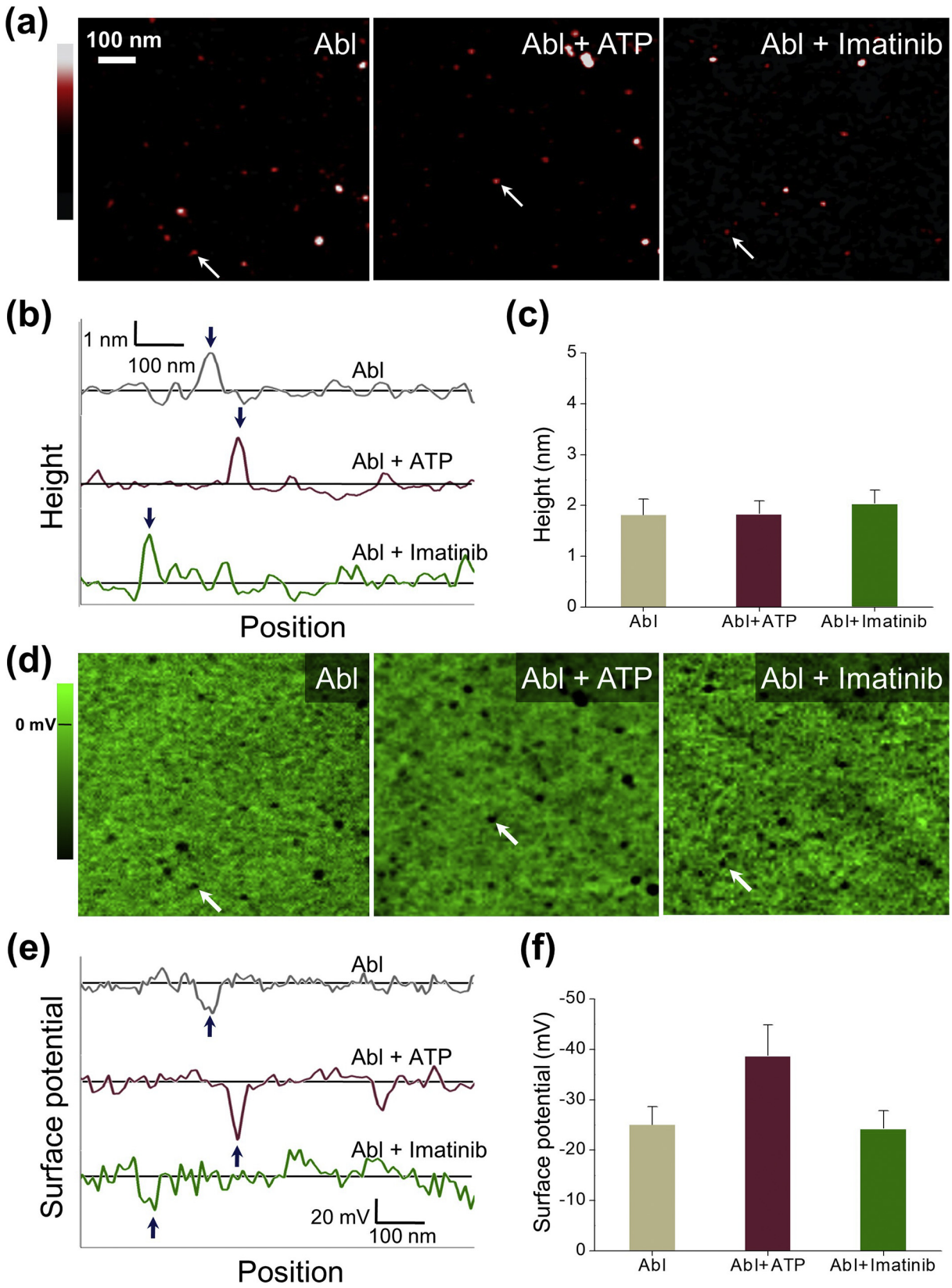

Fig. 4. KPFM imaging-based analysis of interaction between cancer-specific proteins and drug molecules. (a) Tapping mode AFM images of Abl tyrosine kinase (marked as a white arrow) in unbound state (left), ATP-bound state (middle), and imatinib-bound state (right). (b) AFM height profiles of Abl tyrosine kinase in three different states. (c) Average height of imaged Abl tyrosine kinase in three different states. (d) KPFM images of Abl tyrosine kinases (marked as a white arrow) in unbound state (left), ATP-bound state (middle), and imatinib-bound state (right). (e) Surface potential profiles of Abl tyrosine kinases in three different states. (f) Average surface potential of imaged Abl tyrosine kinases in three different states. Figure is adopted with permission from Ref. [21].

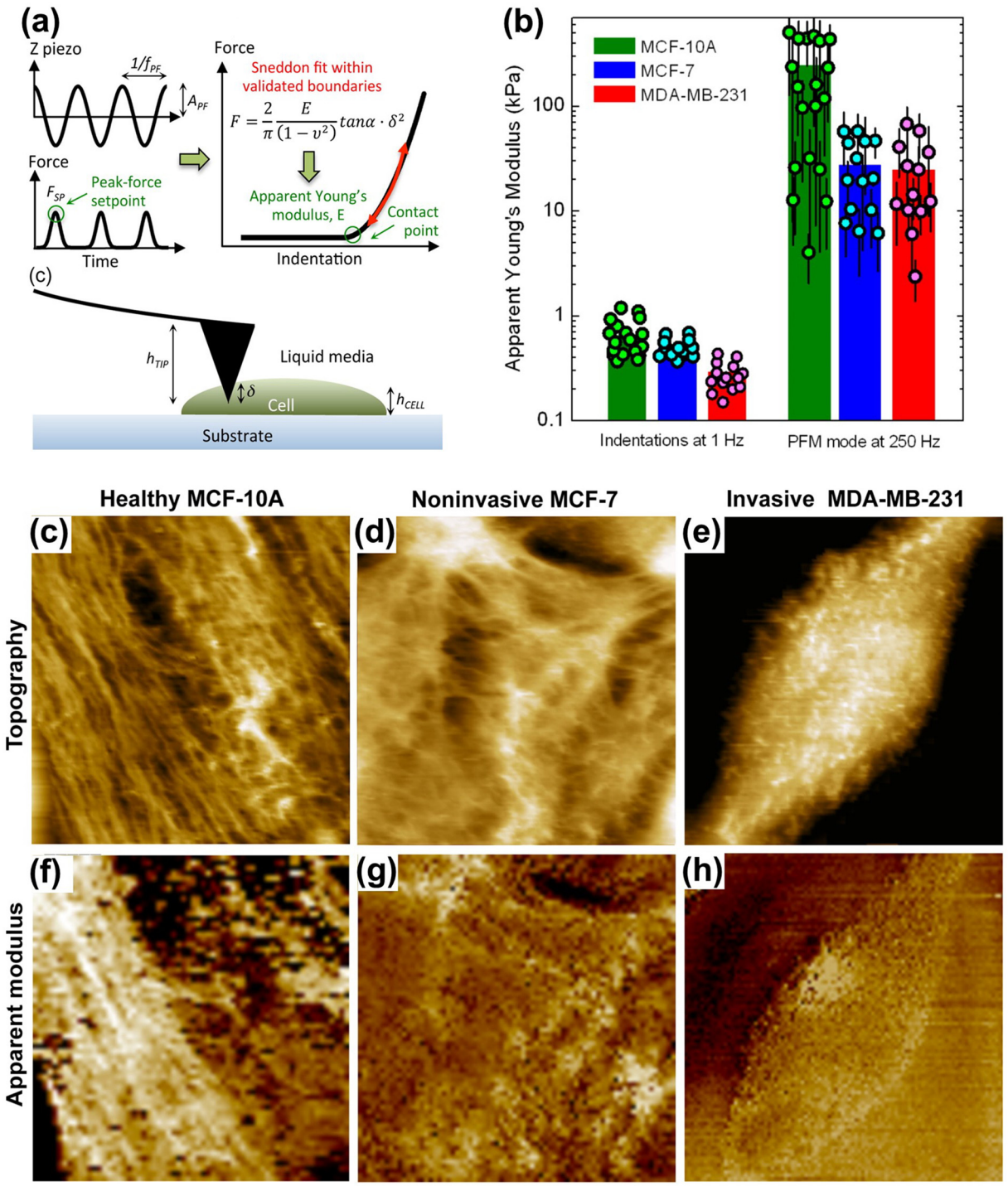

Fig. 5. (a) Schematic representation of the operation of peak-force modulation AFM for imaging live cells. The peak value of the periodic force (F_{SP}) resulting on the tip as a consequence of sinusoidal actuation on the cantilever (at frequency f_{PF} with amplitude A_{PF}) is used for feedback control. Real-time measurements of the force versus tip-sample distance are converted into force-indentation curves that are fitted to Sneddon equation for a conical indenter for obtaining the elastic modulus of live cells. (b) Comparison of average values of Young's modulus for single cells obtained by either low loading rate indentation at 1 Hz or peak-force modulation mode at 250 Hz. (c)–(e) AFM topology images of (c) healthy MCF-10A cell, (d) non-invasive MCF-7 cells, and (e) invasive MDA-MB-231 cells. (f)–(h) Nanomechanical mapping images of (f) healthy MCF-10A cells, (g) non-invasive MCF-7 cells, and (h) invasive MDA-MB-231 cells. Figure is adopted with permission from Ref. [80].

cellular motility and metastasis in highly invasive cancer cells. They examined how the Syk expression affects the physical properties of an invasive breast cancer cell line. The height and elasticity of highly invasive breast carcinoma cells with Syk expression were measured. This study proved that multi-harmonic AFM can help distinguish the nanomechanical properties of live cancer cells from those of normal cells. NMM also enables tracking tumor progression by measuring variations in the cell mechanical properties as a function of metastatic potential.

Cancer progression makes different states of cytoskeleton tension resulting in the change of cell stiffness during cancer development [77–79]. The physical state of cytoskeleton is affected by actin fibers, which are bundles or networks organized within cells. San Paulo et al. [80] reported differences between the stiffness of normal cells and breast cancer cells, which depend on the conformation of the F-actin

cytoskeleton structures. They showed high-resolution tomography and stiffness image of actin filaments within living cells with different degrees of malignancy, such as MCF-10A (healthy), MCF-7 (tumorigenic, non-invasive), and MDA-MD-231 (tumorigenic, invasive) by using peak force modulation AFM (Fig. 5a, c – h). They compared Young's modulus of three cell lines with different degrees of malignancy (Fig. 5b). Moreover, Iyer et al. [81] reported how the mechanical properties of cancerous and normal epithelial cells are determined by using AFM indentation and SEM imaging. It was found that the mechanical properties of cells are dependent on a brush layer on the cell surface. In particular, the distribution and length of brush layer on the surface of epithelial cell determine its mechanical properties in such a way that the different distribution and length of brush layers result in the stiffer cancerous epithelial cells when compared with normal epithelial cells. In addition, the relationship between the elastic property of cells and protein molecules inside cells has been investigated. For instance, Gunning and coworkers [82] found that the elastic modulus of a cell is regulated by tropomyosin isoform composition of actin cytoskeleton inside the cell. Furthermore, how chemical treatment or microenvironment affects the elastic property of cells has been studied. Specifically, Heu et al. [83] studied how chemical treatment of human epithelial cells makes effect on their elastic modulus. It is found that Glyphosate, which is a chemical found to increase the risk of cancer, increases the elastic modulus of epidermal cell. A recent study by Li et al. [84] reports that drug treatment (e.g. using rituximab) results in the first decrease of elastic modulus of cell (e.g. Raji cell) followed by the increase of cell elastic modulus. Since the elastic modulus of tumor cells is found to be related to their uncontrolled division and migration, the drug has to be designed such that the drug can affect the mechanical properties of tumor cells leading to the prevention of cancer cell propagation. A previous study by Guo et al. [85] suggests that microenvironment condition (e.g. cell-to-cell contact) also plays a role in determining the elastic modulus of epithelial cells. Plodinec et al. [86] reported the stiffness map of cancerous (or normal) cells within tumor microenvironment by NMM. The stiffness map of malignant cells obtained from a breast cancer patient shows a broad distribution of elastic modulus with a prominent low-stiffness peaks representing the properties of cancerous cells. This work suggests that NMM of tissue samples (i.e. biopsies) is useful for quantitative diagnosis and prognosis of cancer.

6. Vibrant cantilever-based cancer diagnosis

As described earlier, cantilever-based biomolecular detection can be implemented by measuring the cantilever's bending deflection change [23] or frequency shift [28] due to biomolecular interactions. As the resonant frequency of a cantilever is determined from its mass and stiffness [87], a resonant cantilever is useful in measuring the mass of specific biomolecules. The detection principle of resonant cantilever-based sensing is well described in Section 2.4 and in literatures [25–27,88] including our previous work [28].

Here, we review AFM cantilever-based characterization of enzymatic cleavage due to matrix metalloproteinase (MMP) that is expressed on the surface of cancerous cells [39]. MMP plays a key role in degrading the extracellular matrix, which is necessary for cancer metastasis [89,90]. Fig. 6 shows the schematic illustration of cantilever-based characterization of enzymatic cleavage by membrane type 1-MMP (MT1-MMP). When MT1-MMP interacts with a peptide-immobilized cantilever, the cleavage of peptides functionalized on the cantilever decreases its overall mass, and consequently increases its resonant frequency. The resulting shift in the resonant frequency is represented in the form of $\Delta\omega(t) = \Delta\omega_0[1 - \exp(-k_p t)]$, where k_p is the kinetic rate of enzymatic cleavage, and $\Delta\omega_0$ is the equilibrium (i.e. steady-state) value of the resonant frequency shift. The values of k_p and $\Delta\omega_0$ depend on the MT1-MMP concentration. It is shown that a drug molecule (GM6001) is able to effectively inhibit the MT1-MMP-driven enzymatic cleavage. To evaluate the potential of AFM cantilever for cancer diagnosis, we took into account the cantilever-based detection of the proteolytic activity of MT1-MMP extracted from the membranes of live cancer cells (i.e. HT1080 cells) and them treated with GM6001 or small interfering RNA (siRNA). Though the western blot analysis confirms that siRNA regulates MT1-MMP, the western blot is unable to confirm the ability of GM6001 to regulate the activity of MT1-MMP. However, the vibrant cantilever sensor enables the quantitative characterization of the proteolytic activity of MT1-MMP regulated by both siRNA and GM6001. While the resonant frequency shift is clearly seen for the case of HT1080 cells, the resonant frequency of AFM cantilever is mostly unaffected by injection of cell lysates of HT1080 treated with GM6001. This confirms that GM6001 is able to effectively regulate the proteolytic activity of MT1-MMP. Our previous work [39] sheds light on the cantilever-based detection, which will open a new avenue for fast and point-of-care cancer diagnosis.

To further the realization of cantilever-based cancer diagnosis, we employed a peptide-functionalized cantilever sensor with using a clinically relevant samples such as blood from animals or cancer patients [91]. In particular, we used a cantilever biosensor, whose surface was functionalized with peptides that are able to specifically interact with MMP2, for analyzing the progression of lung cancer. We have shown that the secretion level and proteolytic activity of MMP2 can be quantitatively correlated with not only the type of cancer cells but also the tumor growth state based on the results of cantilever bioassay using animal blood (Fig. 7a–d). Furthermore, cantilever-based diagnosis using the blood droplet of lung cancer patients showed that the amount of frequency shift (proportional to the secretion level of MMP) and the kinetic rate of proteolysis are critically dependent on the level of cancer metastasis, in such a way that the more distant metastasis (or the more spreading of tumors to regional lymph nodes), the higher values of frequency shift and the kinetic rate of proteolytic activity (Fig. 7f–i). This implies that the level of cancer development can be quantitatively analyzed using the AFM cantilever bioassay, which the conventional diagnosis toolkits are unable to do.

In addition to the ability of vibrant cantilever to detect cancer-specific proteins, the cantilever sensor is able to quantitate the dynamics of biological organisms (e.g. virus, bacteria, and cancer cells) and their response to chemical treatment (e.g. drug molecule injection). A previous work by Park et al. [92] showed that a vibrant cantilever sensor is able to measure the mass of cells as well as the change of cell mass during cellular growth. A pioneering work by Longo et al. [93] first reported the metabolic dynamics of bacteria and its response to antibiotics by measuring the bending fluctuation of a cantilever due to the dynamics of the bacteria and also its response to antibiotics. In particular, they studied the metabolic dynamics of *E. coli* as a function of glucose concentration by evaluating the fluctuation of cantilever's bending deflection due to the metabolism of *E. coli*. In a similar spirit, Muller and coworkers [94] employed a cantilever sensor for studying the dynamics of live mammalian cells under their growth and cellular process. They measured the fluctuation of cell mass due to cellular cycle by measuring the frequency behavior of a cantilever sensor, onto which a live mammalian cell was attached. Moreover, it was shown that for a mammalian cell infected with virus, the cell mass is not significantly increased when compared with a wild type mammalian cell, indicating that virus infection arrests the cell growth (Fig. 8). Though a recent study by Muller and coworkers reports the cantilever sensor-based characterization of the dynamics of cells, their method can be further extended for studying the dynamics of live cancer cells and their response to chemical treatment with drug molecule. In other words, cantilever sensor exhibits a great potential in quantitatively studying the properties and dynamics of live cancer cells. Recently, a resonant microchannel-embedded cantilever developed by Manalis and collagues has been shown to be able to measure the increase rate of the mass of single cells during their growth [95] as well as the change of cell mass for tumor cells due to drug treatment [96].

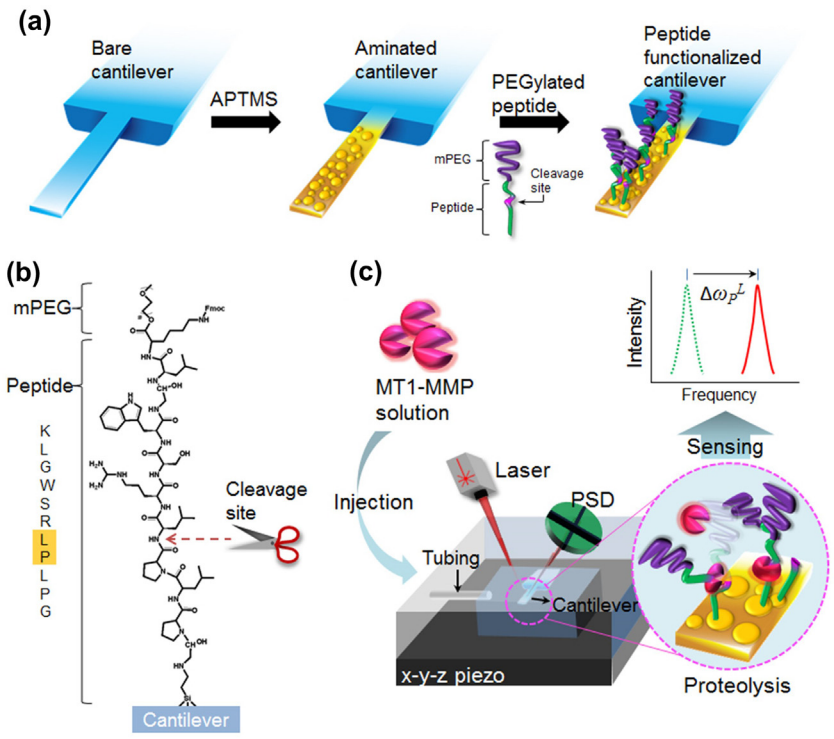

Fig. 6. Schematic illustration of cantilever sensor for detecting the proteolytic activity of membrane type 1-matrix metalloproteinase. (a) Preparation of a peptide-functionalized cantilever. (b) Chemical structure of peptide sequence with cleavage site highlighted in yellow. (c) Experimental setup and sensing mechanisms. APTMS = 3-aminopropyltrimethoxysilane, mPEG = monomethyl poly-(ethylene glycol), PSD = position-sensitive detector. Figure is adopted with permission from Ref. [39].

7. Summary

We have summarized AFM-based imaging and detection for cancer diagnosis, such as AFM/KPFM-based analysis of biomolecular interactions at single-molecule resolution. The high resolution AFM imaging-based analysis helps in the early cancer diagnosis due to its high

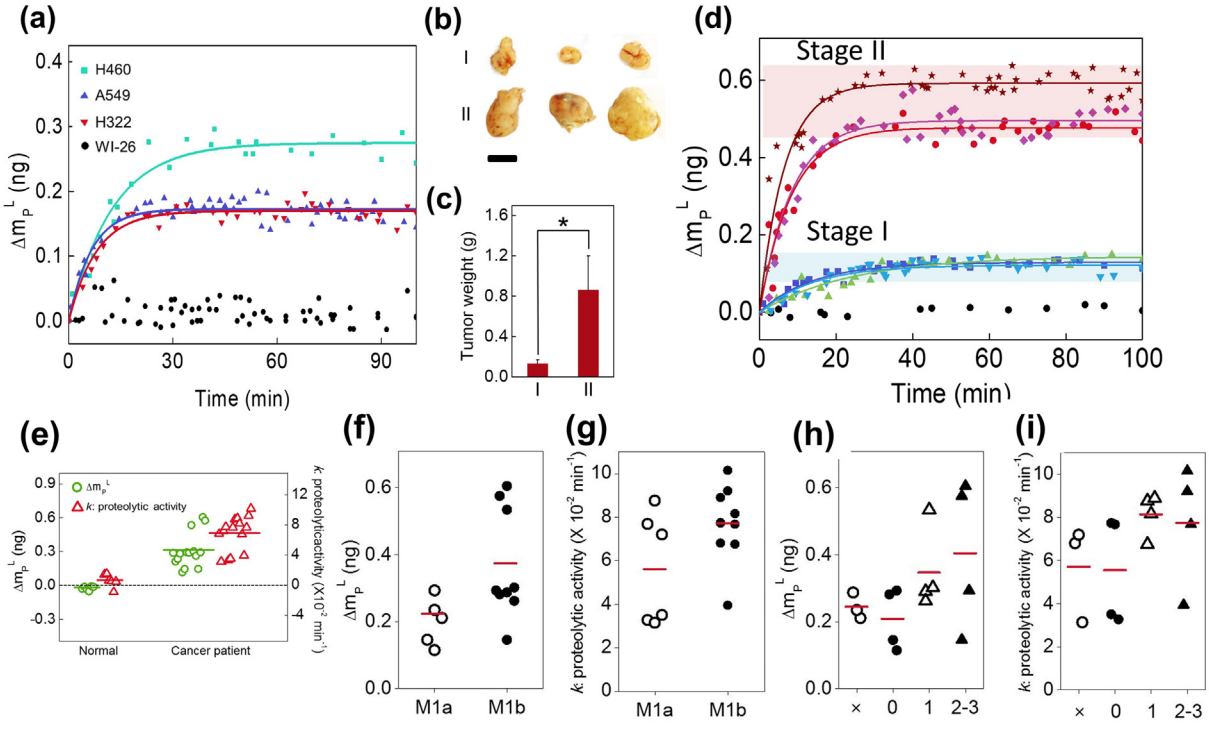

Fig. 7. (a) Nanomechanical detection of MMP2 molecules secreted from cancer cells during their progression. The mass of cleaved peptide chains due to MMP2 molecules that are likely to be secreted from different types of cancer cells such as H460, A549, and H322 cells, respectively. (b) Photographic images of tumors at two different stages, i.e. stage I and II. Scale bar is 10 mm. (c) The weight of tumors at these two different stages. (d) In situ measurement of the mass of cleaved peptides due to MMP2 secreted in the blood of mouse at two different stages. (e) The total mass of cleaved peptides and the kinetic rate of proteolysis due to MMP2 in the blood droplet of cancer patients. (f) The total mass of cleaved peptides with respect to the level of distant metastasis. (g) The kinetic rate of proteolysis as a function of the level of distant metastasis. (h) The total mass of cleaved peptides with respect to the degree of spread to regional lymph node. (i) The kinetic rate of proteolysis as a function of the degree of spread to regional lymph node. Figures are adopted from [91] under Creative Commons Attribution License.

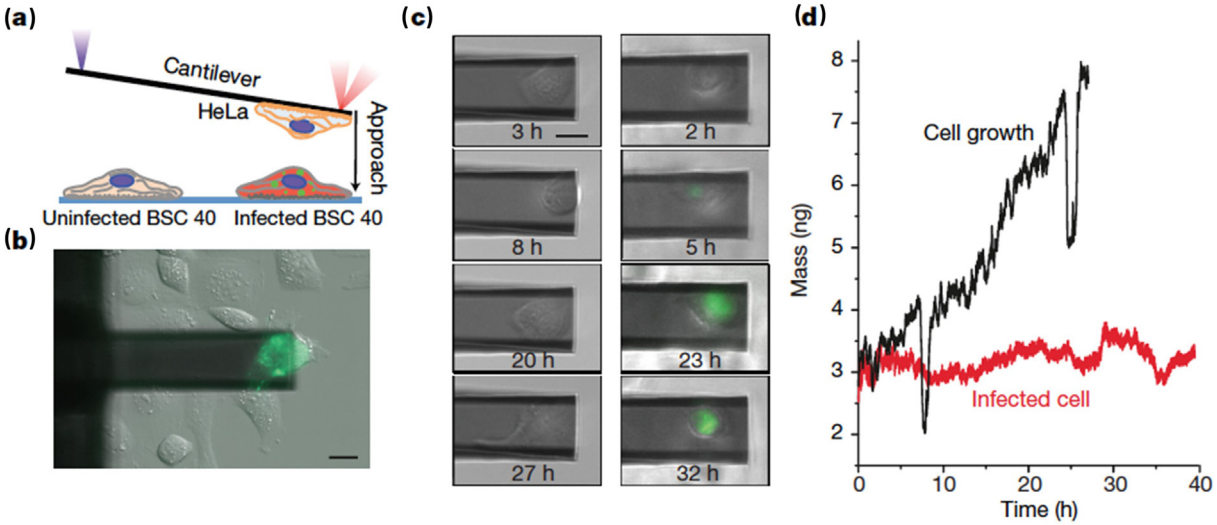

Fig. 8. (a) Schematic illustration of cell-to-cell virus infection. An uninfected HeLa cell, which was attached on the cantilever's surface, is held for 5 min close to the virus-infected BSC40 cell. (b) Fluorescence image of HeLa cell infected with virus on a cantilever's surface. (c) Time-lapse fluorescence images of an uninfected HeLa cell (left) or virus-infected HeLa cell (right) on the cantilever's surface. The fluorescence label eGFP was attached to the virus. (d) The time-dependent cell mass of uninfected HeLa cell (black) or virus-infected HeLa cell (red) under cell growth. Figure is adopted with permission from Ref. [94].

detection sensitivity close to single-molecule level. KPFM imaging-based analysis can help evaluate the ability of a drug molecule to regulate the interaction between a specific protein and a ligand, implying the potential of KPFM imaging as a nanotechnology toolkit for molecular-level drug screening. In addition, as it enables the quantitative characterization of biomolecular binding, the AFM/KPFM imaging-based analysis can be further extended for mapping the binding affinities between various protein molecules. This mapping is of great importance in proteomics to gain insights into the cellular signaling or regulation of such signaling, which determines the cellular functions [97,98].

AFM-based NMM plays an important role in characterizing the physical properties of cancerous cells or tissues. The elasticity of cancer cells is dependent on the distribution of cytoskeleton and actin within a cell or brush layer on the cell surface. Thus AFM NMM allows for quantitatively monitoring the status of cancer, and functions as a nanoscale biopsy at high resolution and precision affording early cancer diagnosis or sensitive cancer prognosis.

Furthermore, AFM cantilever can serve as a nanomechanical bioassay toolkit for quantitative characterization of biomolecular interaction such as enzymatic cleavage (driven by MMP) necessary for cancer diagnosis/prognosis, which the conventional bioassay is unable to do. More importantly, AFM cantilever is able to quantitate the activity of MMP expressed on cancer cells that are regulated by drug molecule. This indicates the ability of cantilever bioassay to quantitate the status of cancerous cells. As the level of cancer progression is highly correlated with the amount of MMP [99] that is able to degrade extracellular matrix environment, the cantilever bioassay is capable of quantitating the level of cancer progression (e.g. tumor growth state or the level of cancer metastasis) by measuring the secretion level and proteolytic activity of MMP released from cancer cells during cancer development. The AFM cantilever bioassay is able to quantitate the level of cancer metastasis using a drop of blood from cancer patients. In addition, AFM cantilever can be employed for studying the dynamics of live cells (including live cancer cells) as well as their response to chemical treatment, which implies a great potential of AFM cantilever for cancer diagnosis and therapeutics.

Here, it should be noted that most of research works introduced in this paper considered the label-free, sensitive detection of cancer-specific biomolecules using a prepared solution (e.g. buffer solution containing biomolecules, solution obtained from cell lysate or cell culture medium, and so forth) rather than clinically relevant samples (e.g. blood, urine, etc.) except our recent study [91] reporting the ability of vibrant cantilever to identify the status of cancer metastasis using a blood droplet of cancer patient. For further application in cancer diagnosis, AFM-based diagnosis has to be extended by considering the clinically relevant samples such as blood droplet (or urine) obtained from cancer patients. In addition, it is still challenging for AFM-based diagnosis to be employed for tracking the status of cancer progression (e.g. metastasis) by quantitating the amount of cancer-specific biomolecules released in blood from tumor cells. We anticipate that AFM-based cancer diagnosis will be further extended for studying the cancer progression, and that AFM-based cancer diagnosis will be added to conventional cancer diagnostic approaches in order to improve the accuracy and acuteness of cancer diagnosis.

Therefore, biomolecular detection based on AFM/KPFM/NMM imaging or vibrant AFM cantilever will play an unprecedented role in cancer diagnosis. The high detection sensitivity of AFM/KPFM imaging, down to 1 pM, allows for early cancer diagnosis, where tracing the amount of specific proteins (e.g. CEA) expressed on tumor cells is required. NMM imaging is able to distinguish cancer cells from normal cells by measuring the physical (mechanical) properties of cells. The AFM cantilever can quantitate the activity of proteinases expressed or secreted from tumor cells, and hence the status of cancer development. AFM cantilever is also capable of quantitating the dynamics of live (cancer) cells and their responses to biochemical treatment. Thus we believe AFM-based detection – both AFM/KPFM/NMM imaging and AFM cantilever – may pave a way for developing a point-of-care and fast diagnostic system enabling the early cancer diagnosis or cancer prognosis.

Conflicts of interest

None.

Funding source

T.K. appreciates the financial support from the National Research Foundation of Korea (NRF) under Grant No. NRF-2015R1A2A1A15052758 and NRF-2017R1D1A1B03031930. K.E. gratefully acknowledges the financial support from NRF under Grant No. NRF-2015R1A2A2A04002453.

References

[1] T. Vos, et al., Global, regional, and national incidence, prevalence, and years lived with disability for 310 diseases and injuries, 1990–2015: a systematic analysis for the Global Burden of Disease Study 2015, Lancet 388 (2016) 1545–1602.
[2] B.W. Stewart, C.P. Wild, World Cancer Report, World Health Organization, Lyon, France, 2014.
[3] J.E. Visvader, Cells of origin in cancer, Nature 469 (2011) 314–322.
[4] A.C. Chiang, J. Massague, Molecular basis of metastasis, N. Engl. J. Med. 359 (2008) 2814–2823.
[5] J.R. Heath, M.E. Davis, Nanotechnology and cancer, Annu. Rev. Med. 59 (2008) 251.
[6] R. Bashir, BioMEMS: state-of-the-art in detection, opportunities and prospects, Adv. Drug Deliv. Rev. 56 (2004) 1565–1586.
[7] H.G. Craighead, Future lab-on-a-chip technologies for interrogating individual molecules, Nature 442 (2006) 387–393.
[8] F. Patolsky, B.T. Timko, G. Zheng, C.M. Lieber, Nanowire-based nanoelectronic devices in the life sciences, MRS Bull. 32 (2007) 142–149.
[9] H.G. Craighead, Nanoelectromechanical systems, Science 290 (2000) 1532–1535.
[10] J. Fritz, M.K. Baller, H.P. Lang, H. Rothuizen, P. Vettiger, E. Meyer, H.J. Guntherodt, C. Gerber, J.K. Gimzewski, Translating biomolecular recognition into nanomechanics, Science 288 (2000) 316–318.
[11] D.J. Muller, Y.F. Dufrene, Atomic force microscopy as a multifunctional molecular toolbox in nanobiotechnology, Nat. Nanotechnol. 3 (2008) 261–269.
[12] F.J. Giessibl, C.F. Quate, Exploring the nanoworld with atomic force microscopy, Phys. Today 59 (2006) 44–50.
[13] H.G. Hansma, Surface biology of DNA by atomic force microscopy, Annu. Rev. Phys. Chem. 52 (2001) 71–92.
[14] M. Nonnenmacher, M.P. O'Boyle, H.K. Wickramasinghe, Kelvin probe force microscopy, Appl. Phys. Lett. 58 (1991) 2921–2923.
[15] G.H. Enevoldsen, T. Glatzel, M.C. Christensen, J.V. Lauritsen, F. Besenbacher, Atomic scale Kelvin probe force microscopy studies of the surface potential variations on the TiO_2(110) surface, Phys. Rev. Lett. 100 (2008) 236104.
[16] M.E. Dickinson, J.P. Schirer, Probing more than the surface, Mater. Today 12 (2009) 46–50.
[17] Y.-S. Sohn, J. Park, G. Yoon, S.-W. Jee, J.-H. Lee, S. Na, T. Kwon, K. Eom, Mechanical properties of silicon nanowires, Nanoscale Res. Lett. 5 (2010) 211–216.
[18] A. Gouldstone, N. Chollacoop, M. Dao, J. Li, A.M. Minor, Y.-L. Shen, Indentation across size scales and disciplines: Recent developments in experimentation and modeling, Acta Mater. 55 (2007) 4015–4039.
[19] O.K. Wong, M. Guthold, D.A. Erie, J. Gelles, Interconvertible lac repressor-DNA loops revealed by single-molecule experiments, PLoS Biol. 6 (2008) e232.
[20] D.C. Hansen, K.M. Hansen, T.L. Ferrell, T. Thundat, Discerning biomolecular interactions using Kelvin probe technology, Langmuir 19 (2003) 7514–7520.
[21] J. Park, J. Yang, G. Lee, C.Y. Lee, S. Na, S.W. Lee, S. Haam, Y.-M. Huh, D.S. Yoon, K. Eom, T. Kwon, Single-molecule recognition of biomolecular interaction via Kelvin probe force microscopy, ACS Nano 5 (2011) 6981–6990.
[22] O. Sahin, S. Magonov, C. Su, C.F. Quate, O. Solgaard, An atomic force microscope tip designed to measure time-varying nanomechanical forces, Nat. Nanotechnol. 2 (2007) 507–514.
[23] K.M. Goeders, J.S. Colton, L.A. Bottomley, Microcantilevers: sensing chemical interactions via mechanical motion, Chem. Rev. 108 (2008) 522–542.
[24] A. Boisen, T. Thundat, Design & fabrication of cantilever array biosensors, Mater. Today 12 (2009) 32–38.
[25] R. Datar, S. Kim, S. Jeon, P. Hesketh, S. Manalis, A. Boisen, T. Thundat, Cantilever sensors: nanomechanical tools for diagnostics, MRS Bull. 34 (2009) 449–454.
[26] A. Boisen, S. Dohn, S.S. Keller, S. Schmid, M. Tenje, Cantilever-like micromechanical sensors, Rep. Prog. Phys. 74 (2011) 036101.
[27] J.L. Arlett, E.B. Myers, M.L. Roukes, Comparative advantages of mechanical biosensors, Nat. Nanotechnol. 6 (2011) 203–215.
[28] K. Eom, H.S. Park, D.S. Yoon, T. Kwon, Nanomechanical resonators and their applications in biological/chemical detection: nanomechanics principles, Phys. Rep. 503 (2011) 115–163.
[29] P.S. Waggoner, H.G. Craighead, Micro- and nanomechanical sensors for environmental, chemical, and biological detection, Lab Chip 7 (2007) 1238–1255.
[30] R. McKendry, J.Y. Zhang, Y. Arntz, T. Strunz, M. Hegner, H.P. Lang, M.K. Baller, U. Certa, E. Meyer, H.J. Guntherodt, C. Gerber, Multiple label-free biodetection and quantitative DNA-binding assays on a nanomechanical cantilever array, Proc. Natl. Acad. Sci. U. S. A. 99 (2002) 9783–9788.
[31] T. Kwon, K. Eom, J. Park, D.S. Yoon, H.L. Lee, T.S. Kim, Micromechanical observation of the kinetics of biomolecular interactions, Appl. Phys. Lett. 93 (2008) 173901.
[32] G.H. Wu, H.F. Ji, K. Hansen, T. Thundat, R. Datar, R. Cote, M.F. Hagan, A.K. Chakraborty, A. Majumdar, Origin of nanomechanical cantilever motion generated from biomolecular interactions, Proc. Natl. Acad. Sci. U. S. A. 98 (2001) 1560–1564.
[33] T.Y. Kwon, K. Eom, J.H. Park, D.S. Yoon, T.S. Kim, H.L. Lee, In situ real-time monitoring of biomolecular interactions based on resonating microcantilevers immersed in a viscous fluid, Appl. Phys. Lett. 90 (2007) 223903.
[34] G.H. Wu, R.H. Datar, K.M. Hansen, T. Thundat, R.J. Cote, A. Majumdar, Bioassay of prostate-specific antigen (PSA) using microcantilevers, Nat. Biotechnol. 19 (2001) 856–860.
[35] P.S. Waggoner, M. Varshney, H.G. Craighead, Detection of prostate specific antigen with nanomechanical resonators, Lab Chip 9 (2009) 3095–3099.
[36] J. Zhang, H.P. Lang, F. Huber, A. Bietsch, W. Grange, U. Certa, R. McKendry, H.J. Guntherodt, M. Hegner, C. Gerber, Rapid and label-free nanomechanical detection of biomarker transcripts in human RNA, Nat. Nanotechnol. 1 (2006) 214–220.
[37] Y. Weizmann, R. Elnathan, O. Lioubashevski, I. Willner, Magnetomechanical detection of the specific activities of endonucleases by cantilevers, Nano Lett. 5 (2005) 741–744.
[38] T. Kwon, J. Park, J. Yang, D.S. Yoon, S. Na, C.-W. Kim, J.S. Suh, Y.M. Huh, S. Haam, K. Eom, Nanomechanical in situ monitoring of proteolysis of peptide by cathepsin B, PLoS One 4 (2009) e6248.
[39] G. Lee, K. Eom, J. Park, J. Yang, S. Haam, Y.-M. Huh, J.K. Ryu, N.H. Kim, J.I. Yook, S.W. Lee, D.S. Yoon, T. Kwon, Real-time quantitative monitoring of specific peptide cleavage by a proteinase for cancer diagnosis, Angew. Chem. Int. Ed. 51 (2012) 5837–5841.
[40] W.J. Greenleaf, M.T. Woodside, S.M. Block, High-resolution, single-molecule measurements of biomolecular motion, Annu. Rev. Biophys. Biomol. Struct. 36 (2007) 171–190.
[41] Y.F. Dufrene, Towards nanomicrobiology using atomic force microscopy, Nat. Rev. Microbiol. 6 (2008) 674–680.
[42] C.M. Dobson, Protein folding and misfolding, Nature 426 (2003) 884–890.
[43] G. Lee, W. Lee, H. Lee, S.W. Lee, D.S. Yoon, K. Eom, T. Kwon, Mapping the surface charge distribution of amyloid fibril, Appl. Phys. Lett. 101 (2012) 043703.
[44] G. Lee, W. Lee, H. Lee, C.Y. Lee, K. Eom, T. Kwon, Self-assembled amyloid fibrils with controllable conformational heterogeneity, Sci. Rep. 5 (2015) 16220.
[45] G. Yoon, M. Lee, J.I. Kim, S. Na, K. Eom, Role of sequence and structural polymorphism on the mechanical properties of amyloid fibrils, PLoS One 9 (2014) e88502.
[46] M.B. Pepys, Amyloidosis, Annu. Rev. Med. 57 (2006) 223–241.
[47] G. Merlini, V. Bellotti, Molecular mechanisms of amyloidosis, N. Engl. J. Med. 349 (2003) 583–596.
[48] F. Chiti, C.M. Dobson, Protein misfolding, functional amyloid, and human disease, Annu. Rev. Biochem. 75 (2006) 333–366.
[49] K.L. Johnson, Contact Mechanics, Cambridge University Press, 1987.
[50] E.U. Azeloglu, K.D. Costa, Atomic force microscopy in mechanobiology: measuring microelastic heterogeneity of living cells, in: P. Braga, D. Ricci (Eds.), Atomic Force Miicroscopy in Biomedical Research: Methods and Protocols, Springer, New York, 2011, pp. 303–329.
[51] K. Haase, A.E. Pelling, Investigating cell mechanics with atomic force microscopy, J. R. Soc. Interf. 12 (2015) 20140970.
[52] G. Bao, S. Suresh, Cell and molecular mechanics of biological materials, Nat. Mater. 2 (2003) 715.
[53] E. Moeendarbary, A.R. Harris, Cell mechanics: principles, practices, and prospects, Wiley Interdiscip. Rev. Syst. Biol. Med. 6 (2014) 371–388.
[54] N. The Physical Sciences - Oncology Centers, A physical sciences network characterization of non-tumorigenic and metastatic cells, Sci. Rep. 3 (2013) 1449.
[55] M. Yilmaz, G. Christofori, EMT, the cytoskeleton, and cancer cell invasion, Cancer Metastasis Rev. 28 (2009) 15–33.
[56] L.T. Mazzola, S.P. Fodor, Imaging biomolecule arrays by atomic force microscopy, Biophys. J. 68 (1995) 1653–1660.
[57] A.L. Weisenhorn, B. Drake, C.B. Prater, S.A. Gould, P.K. Hansma, F. Ohnesorge, M. Egger, S.P. Heyn, H.E. Gaub, Immobilized proteins in buffer imaged at molecular resolution by atomic force microscopy, Biophys. J. 58 (1990) 1251–1258.
[58] J.L. Huff, M.P. Lynch, S. Nettikadan, J.C. Johnson, S. Vengasandra, E. Henderson, Label-free protein and pathogen detection using the atomic force microscope, J. Biomol. Screen. 9 (2004) 491–497.
[59] K.-B. Lee, E.-Y. Kim, C.A. Mirkin, S.M. Wolinsky, The use of nanoarrays for highly sensitive and selective detection of human immunodeficiency virus type 1 in plasma, Nano Lett. 4 (2004) 1869–1872.
[60] K. Nam, K. Eom, J. Yang, J. Park, G. Lee, K. Jang, H. Lee, S.W. Lee, D.S. Yoon, C.Y. Lee, T. Kwon, Aptamer-functionalized nano-pattern based on carbon nanotube for sensitive, selective protein detection, J. Mater. Chem. 22 (2012) 23348–23356.
[61] S. Wang, K. Liu, J. Liu, Z.T.-F. Yu, X. Xu, L. Zhao, T. Lee, E.K. Lee, J. Reiss, Y.-K. Lee, L.W.K. Chung, J. Huang, M. Rettig, D. Seligson, K.N. Duraiswamy, C.K.-F. Shen, H.-R. Tseng, Highly efficient capture of circulating tumor cells by using nanostructured silicon substrates with integrated chaotic micromixers, Angew. Chem. Int. Ed. 50 (2011) 3084–3088.
[62] S. Nagrath, L.V. Sequist, S. Maheswaran, D.W. Bell, D. Irimia, L. Ulkus, M.R. Smith, E.L. Kwak, S. Digumarthy, A. Muzikansky, P. Ryan, U.J. Balis, R.G. Tompkins, D.A. Haber, M. Toner, Isolation of rare circulating tumour cells in cancer patients by microchip technology, Nature 450 (2007) 1235.
[63] N. Vardakis, I. Messaritakis, C. Papadaki, G. Agoglossakis, M. Sfakianaki, Z. Saridaki, S. Apostolaki, I. Koutroubakis, M. Perraki, D. Hatzidaki, D. Mavroudis, V. Georgoulias, J. Souglakos, Prognostic significance of the detection of peripheral blood CEACAM5mRNA-positive cells by real-time polymerase chain reaction in operable colorectal cancer, Clin. Cancer Res. 17 (2011) 165–173.
[64] M.C. Miller, G.V. Doyle, L.W.M.M. Terstappen, Significance of circulating tumor cells detected by the CellSearch system in patients with metastatic breast colorectal and prostate cancer, J. Oncol. 2010 (2010).
[65] C. Aggarwal, E. Mitchell, M.C. Miller, S.J. Cohen, N.J. Meropol, C.J. Punt, N. Iannotti, B.H. Saidman, K.D. Sabbath, N.Y. Gabrail, J. Picus, M.A. Morse, Relationship among circulating tumor cells, CEA and overall survival in patients with metastatic colorectal cancer, Ann. Oncol. 24 (2012) 420–428.
[66] T. Kwon, J. Park, G. Lee, K. Nam, Y.-M. Huh, S.-W. Lee, J. Yang, C.Y. Lee, K. Eom, Carbon nanotube-patterned surface-based recognition of carcinoembryonic antigens in tumor cells for cancer diagnosis, J. Phys. Chem. Lett. 4 (2013) 1126–1130.
[67] K. Salaita, Y. Wang, C.A. Mirkin, Applications of dip-pen nanolithography, Nat. Nanotechnol. 2 (2007) 145–155.

[68] A.K. Sinensky, A.M. Belcher, Label-free and high-resolution protein/DNA nanoarray analysis using Kelvin probe force microscopy, Nat. Nanotechnol. 2 (2007) 653–659.
[69] H. Lee, S.W. Lee, G. Lee, W. Lee, J.H. Lee, K.S. Hwang, J. Yang, S.W. Lee, D.S. Yoon, Kelvin probe force microscopy of DNA-capped nanoparticles for single-nucleotide polymorphism detection, Nanoscale 8 (2016) 13537–13544.
[70] K. Jang, J. Choi, C. Park, S. Na, Label-free and high-sensitive detection of Kirsten rat sarcoma viral oncogene homolog and epidermal growth factor receptor mutation using Kelvin probe force microscopy, Biosens. Bioelectron. 87 (2017) 222–228.
[71] K. Bhadriraju, L.K. Hansen, Extracellular matrix- and cytoskeleton-dependent changes in cell shape and stiffness, Exp. Cell Res. 278 (2002) 92–100.
[72] D.E. Discher, P. Janmey, Y.-l. Wang, Tissue cells feel and respond to the stiffness of their substrate, Science 310 (2005) 1139–1143.
[73] S.E. Cross, Y.-S. Jin, J. Rao, J.K. Gimzewski, Nanomechanical analysis of cells from cancer patients, Nat. Nanotechnol. 2 (2007) 780–783.
[74] A.X. Cartagena-Rivera, W.-H. Wang, R.L. Geahlen, A. Raman, Fast, multi-frequency, and quantitative nanomechanical mapping of live cells using the atomic force microscope, Sci. Rep. 5 (2015) 11692.
[75] A. Raman, S. Trigueros, A. Cartagena, A.P.Z. Stevenson, M. Susilo, E. Nauman, S.A. Contera, Mapping nanomechanical properties of live cells using multi-harmonic atomic force microscopy, Nat. Nanotechnol. 6 (2011) 809–814.
[76] M.O. Krisenko, A. Cartagena, A. Raman, R.L. Geahlen, Nanomechanical property maps of breast cancer cells as determined by multiharmonic atomic force microscopy reveal Syk-dependent changes in microtubule stability mediated by MAP1B, Biochemistry 54 (2015) 60–68.
[77] A. Fritsch, M. Hockel, T. Kiessling, K.D. Nnetu, F. Wetzel, M. Zink, J.A. Kas, Are biomechanical changes necessary for tumour progression? Nat. Phys. 6 (2010) 730–732.
[78] D. Wirtz, K. Konstantopoulos, P.C. Searson, The physics of cancer: the role of physical interactions and mechanical forces in metastasis, Nat. Rev. Cancer 11 (2011) 512.
[79] F. Michor, J. Liphardt, M. Ferrari, J. Widom, What does physics have to do with cancer? Nat. Rev. Cancer 11 (2011) 657.
[80] A. Calzado-Martin, M. Encinar, J. Tamayo, M. Calleja, A. San Paulo, Effect of actin organization on the stiffness of living breast cancer cells revealed by peak-force modulation atomic force microscopy, ACS Nano 10 (2016) 3365–3374.
[81] S. Iyer, R.M. Gaikwad, V. Subba Rao, C.D. Woodworth, I. Sokolov, Atomic force microscopy detects differences in the surface brush of normal and cancerous cells, Nat. Nanotechnol. 4 (2009) 389–393.
[82] I. Jalilian, C. Heu, H. Cheng, H. Freittag, M. Desouza, J.R. Stehn, N.S. Bryce, R.M. Whan, E.C. Hardeman, T. Fath, G. Schevzov, P.W. Gunning, Cell elasticity is regulated by the tropomyosin isoform composition of the actin cytoskeleton, PLoS One 10 (2015) e0126214.
[83] C. Heu, A. Berquand, C. Elie-Caille, L. Nicod, Glyphosate-induced stiffening of HaCaT keratinocytes, a peak force tapping study on living cells, J. Struct. Biol. 178 (2012) 1–7.
[84] M. Li, L.-q. Liu, N. Xi, Y.-c. Wang, Nanoscale monitoring of drug actions on cell membrane using atomic force microscopy, Acta Pharmacol. Sin. 36 (2015) 769.
[85] X. Guo, K. Bonin, K. Scarpinato, M. Guthold, The effect of neighboring cells on the stiffness of cancerous and non-cancerous human mammary epithelial cells, N. Z. J. Physiother. 16 (2014) 105002.
[86] M. Plodinec, M. Loparic, C.A. Monnier, E.C. Obermann, R. Zanetti-Dallenbach, P. Oertle, J.T. Hyotyla, U. Aebi, M. Bentires-Alj, Y.H. LimRoderick, C.-A. Schoenenberger, The nanomechanical signature of breast cancer, Nat. Nanotechnol. 7 (2012) 757–765.
[87] L. Meirovitch, Analytical methods in vibrations, Macmillan, New York, 1967.
[88] L.G. Carrascosa, M. Moreno, M. Alvarez, L.M. Lechuga, Nanomechanical biosensors: a new sensing tool, TrAC Trends Anal. Chem. 25 (2006) 196–206.
[89] M. Egebald, Z. Werb, New functions for the matrix metalloproteinases in cancer progression, Nat. Rev. Cancer 2 (2002) 161–174.
[90] L.M. Coussens, B. Fingleton, L.M. Matrisian, Matrix metalloproteinase inhibitors and cancer: trials and tribulatioins, Science 295 (2002) 2387–2392.
[91] J.W. Choi, H. Lee, G. Lee, Y.R. Kim, M.-J. Ahn, H.J. Park, K. Eom, T. Kwon, Blood droplet-based cancer diagnosis via proteolytic activity measurement in cancer progression, Theranostics 7 (2017) 2878–2887.
[92] K. Park, L.J. Millet, N. Kim, H. Li, X. Jin, G. Popescu, N.R. Aluru, K.J. Hsia, R. Bashir, Measurement of adherent cell mass and growth, Proc. Natl. Acad. Sci. U. S. A. 107 (2010) 20691–20696.
[93] G. Longo, L. Alonso-Sarduy, L.M. Rio, A. Bizzini, A. Trampuz, J. Notz, G. Dietler, S. Kasas, Rapid detection of bacterial resistance to antibiotics using AFM cantilevers as nanomechanical sensors, Nat. Nanotechnol. 8 (2013) 522–526.
[94] D. Martínez-Martín, G. Fläschner, B. Gaub, S. Martin, R. Newton, C. Beerli, J. Mercer, C. Gerber, D.J. Müller, Inertial picobalance reveals fast mass fluctuations in mammalian cells, Nature 550 (2017) 500–505.
[95] N. Cermak, S. Olcum, F.F. Delgado, S.C. Wasserman, K.R. Payer, M. A Murakami, S.M. Knudsen, R.J. Kimmerling, M.M. Stevens, Y. Kikuchi, A. Sandikci, M. Ogawa, V. Agache, F. Baleras, D.M. Weinstock, S.R. Manalis, High-throughput measurement of single-cell growth rates using serial microfluidic mass sensor arrays, Nat. Biotechnol. 34 (2016) 1052–1059.
[96] M.M. Stevens, C.L. Maire, N. Chou, M.A. Murakami, D.S. Knoff, Y. Kikuchi, R.J. Kimmerling, H. Liu, S. Haidar, N.L. Calistri, N. Cermak, S. Olcum, N.A. Cordero, A. Idbaih, P.Y. Wen, D.M. Weinstock, K.L. Ligon, S.R. Manalis, Drug sensitivity of single cancer cells is predicted by changes in mass accumulation rate, Nat. Biotechnol. 34 (2016) 1161–1167.
[97] J.S. Sebolt-Leopold, J.M. English, Mechanisms of drug inhibition of signalling molecules, Nature 441 (2006) 457–462.
[98] R.G. Smock, L.M. Gierasch, Sending signals dynamically, Science 324 (2009) 198–203.
[99] S. Garbisa, G. Scagliotti, L. Masiero, C. Di Francesco, C. Caenazzo, M. Onisto, M. Micela, W.G. Stetler-Stevenson, L.A. Liotta, Correlation of serum metalloproteinase levels with lung cancer metastasis and response to therapy, Cancer Res. 52 (1992) 4548–4549.